Title	Drained monotonic responses of suffusional cohesionless soils
Authors	Lin Ke, Akihiro Takahashi
Citation	Journal of Geotechnical and Geoenvironmental Engineering, Vol. 141, Issue 8, 4015033
Pub. date	2015, 8
Copyright	(c) 2015 American Society of Civil Engineers
Note	This material may be downloaded for personal use only. Any other use requires prior permission of the American Society of Civil Engineers. This material may be found at http://dx.doi.org/10.1061/(ASCE)GT.1943-5606.0001327.
Note	This file is author (final) version.

Drained monotonic responses of suffusional cohesionless soils

Lin Ke[1] and Akihiro Takahashi[2]

Abstract

Mechanical consequences of suffusion on the non-cohesive soils with various initial fines contents under different initial effective confining pressures are presented in this paper. By use of the modified triaxial permeameter, seepage tests and successive drained monotonic compression tests are performed. It is found that soil drained strength decreases after suffusion and a temporary drop in stiffness at the initial stage of shearing with respect to the axial strain ranging from 0% ~ 1% is observed. The tests suggest that suffusion might create a distinct packing of soil grains, which might result from possible accumulation of fine grains at the spots where the constriction size, representing the size of pore channels in a soil, is smaller than that of fines. Those "surviving" fines after suffusion may function as reinforcement or jamming at the subsequent compression, resulting in a larger initial stiffness of the suffusional soils.

Keywords: suffusion; drained response; cohesionless soil; soil packing

Journal of Geotechnical and Geoenvironmental Engineering, 141(8), 04015033, 2015

Original URL:

http://dx.doi.org/10.1061/(ASCE)GT.1943-5606.0001327

[1] Postdoctoral Researcher, Department of Civil Engineering, Tokyo Institute of Technology, 2-12-1 Ookayama, Meguro, Tokyo 152-8552, Japan. E-mail: tsingtaolin@gmail.com
[2] Professor, Department of Civil Engineering, Tokyo Institute of Technology, 2-12-1 Ookayama, Meguro, Tokyo 152-8552, Japan (corresponding author). E-mail: takihiro@cv.titech.ac.jp

Introduction

The phenomenon of suffusion in cohesionless soils exhibits itself as the gradual migration of fine grains through the voids of the coarse matrix, transported by volumes of seepage water. It is frequently detected in natural deposit and in earthen structures. The chronic process of suffusion always accompanies with the significant dislodgement of soil grains and changes in hydraulic conductivity. Suffusion may result in a loose soil structure because of the loss of fine grains without great changes in the voids of the coarse matrix. The stress ~ strain relationship of the suffusional soil might be greatly altered compared with the soil without suffusion. There is a high possibility that the strength of the post-suffusion soil decreases due to the destructive function of suffusion. Sugita *et al.* (2008) reported flow slide of several embankments constructed on catchment topography (i.e., swamps and valleys) during Noto Peninsula Earthquake of Japan. Because of the ground configuration, those embankments may have been suffering from years of suffusion and chronically become too weak to resist seismic shakings.

Although soil suffusion might be a huge threat for the stability of existing earthen structures, unfortunately, few studies could comprehensively investigate the consequences of soil suffusion from the perspective of soil mechanics. Chang and Zhang (2011) conducted drained monotonic compression tests on a series of suffusional soil specimens in a revised triaxial apparatus at different stress states. They concluded that the originally dilative soil would become contractive after the loss of significant amounts of fine grains and the drained strength decreased after the suffusion. Undrained monotonic compression tests on internally eroded soil have been performed by Xiao and Shwiyhat (2012). They illustrated that the peak deviator stress of suffusional soil was larger than that of the soil without suffusion, which may be attributed to the low degree of saturation. Chang and Meidani (2012) classified the mechanical behavior of suffusional soil into two categories depending on the confining pressure when suffusion occurs. For the soil specimens that suffered suffusion under low confining pressure, the post-suffusion void ratio was on the dense side of the steady state line in void ratio ~ mean effective stress space, indicating a dilative response, whereas those specimens that experienced suffusion under large confining pressure showed much contractive response with a lower undrained strength. The mechanical consequences of suffusion on soil seem to be obscure, which probably is due to the low saturation degree of the tested specimens after suffusion. Xiao and Shwiyhat (2012) noted that the B-value of the eroded soil specimens immediately after suffusion was approximately 0.86. The complicated unsaturated soil behavior may produce confusing results. Therefore, further detailed testing with the accurate measurements of pressures is necessary to elaborate the mechanical behavior of eroded soil. Meanwhile, models for assessing the mechanical consequences of suffusion have been proposed by Muir Wood *et al*. (2010). In their approach, the progress of suffusion was approximated by progressively removing of grains from the assemblies of circular discs at different stages of shearing. The modelling indicated that the suffusion would alter the soil state from “dense” to “loose”. Hicher (2013) predicted the mechanical behavior of granular materials subjected to particle removal by a micromechanics-based model and concluded that erosion of soils may trigger diffuse failure in an earthen structure.

Full comprehension of the post-suffusion soil behavior is beneficial for the assessment of the stability of potentially eroded earthen structures, such as levees. This study mainly discusses the mechanical consequences of suffusion on non-cohesive soils. By utilizing the modified triaxial permeameter, drained monotonic compression tests are performed on the suffusional specimens, which would be helpful to understand the mechanical characteristics of suffusional cohesionless soil.

Experimental investigations

The experimental investigations are performed using a modified triaxial permeameter, which is capable of directly investigating not only the mechanism of suffusion but also the corresponding change of soil mechanical behaviors induced by erosion of fine grains. Detailed descriptions of the permeameter could be referred to Ke and Takahashi (2014).

Test materials

In this study, the tested sand includes two types of silica sand (Silica No.3 and No.8) with the same specific gravity of 2.645 but different dominant grain sizes (Ke and Takahashi 2012). They are commercially available sands, frequently used as industrial polishing materials. The siliceous sand is mainly composed by quartz, categorized as sub-rounded to sub-angular material. Before testing, they are fully washed and dried to remove impurities. The grain size distributions of Silica No.3 and No.8 are plotted in Fig. 1. Silica No.3 and No.8 correspond to medium sand and fine sand, respectively (ASTM D2487-11). With larger grain size, Silica No.3 works as the coarse fractions which are regarded as soil skeleton in the mixture, whereas Silica No.8 is the erodible fine grains. Hereafter, without specification, the term “fine grains” is referred to Silica No.8 for simplicity. The tested specimens are the binary mixtures of the two sands by three different fines contents (percentage of mass ratios of fine grains to total weight of soil specimen, *FC*), which are 35%, 25% and 15%. The grain size distributions of the mixtures are shown in Fig. 1 indicating that all of the three specimens are gap-graded. The vulnerability of tested specimens to suffusion are assessed by Kezdi’s method (Kezdi, 1979), which indicates internally unstable characteristic of tested soils

($(D_{15c}/d_{85f})_{gap}$=7.9>4, where D_{15c} is the particle size at 15% by passing is finer of Silica No.3 (mm) and d_{85f} refers to the particle size at 85% by passing is finer of Silica No.8 (mm)). Maximum and Minimum void ratios (e_{max} and e_{min}) of tested soil are summarized in Table 1, showing that an increasing in the fines content results in a proportional reduction of e_{max} and e_{min} within 0~35% fines content. This type of binary mixture is commonly referred as "coarse domain soil" and the mechanical responses are largely dependent on the coarse fractions (Lade *et al.*, 1998; Cubrinovski and Ishihara, 2002).

A summary of the test cases is shown in Table 2, where initial void ratio refers to the void ratio of tested specimens under an effective confining pressure of 20kPa prior to consolidation. Each specimen is prepared by moist tamping method that soil mixtures with an initial moisture content of 10% are tamped to the target void ratio to avoid the segregation of the two kinds of grains with different dominant sizes. A non-linear average undercompaction criterion (Jiang *et al.*, 2003) is adopted to generate uniform soil specimens. The tamping on each specimen is in a systematic manner to guarantee an identical input energy. The mean effective stress at consolidation considered in this paper is 50kPa, 100kPa and 200kPa, which approximately corresponds to the vertical effective stress at 5m, 10m and 20m depth, respectively, on condition that groundwater table is at the ground surface and soil ground is fully saturated. Some of the specimens experience suffusion at a constant inflow rate of 5.17×10^{-6}m^3/s in the modified triaxial cell.

Test program

The initial diameter and height of the moist tamped specimens prior to saturation is approximately 70mm and 150mm, respectively. Necessary corrections, such as the effects of buoyancy of the cap and soil, and membrane stiffness, have been considered. Overall, the test program includes soil preparation, vacuum saturation, consolidation, seepage test and compression test. A schematic diagram of the test procedure in the *p'*-*q* stress space (mean effective stress ~ deviator stress) is presented in Fig. 2. Vacuum saturation procedure (ASTM D4767-11) is utilized to saturate the soil specimens. Approximately, the deaerated water with a volume of 10.4 (normalized value in terms of pore volume) has been flowed through the soil specimen. For the majority of tests, B values of at least 0.95 could be achieved after the applying of 100kPa back pressure following the vacuum saturation procedure. The axial displacement and average radial displacement have been recorded all the way to update the present dimension of tested specimens. Upon completion of saturation, soil specimens are isotropically consolidated until the preferred mean effective stress (i.e., 50kPa, 100kPa or 200kPa in this study) is reached. Seepage tests are performed at the stress state the same as that of the specimen after isotropic consolidation. To demonstrate the mechanical effects of suffusion on soils systematically, the imposed inflow rate for each specimen keeps constant as $5.17\times10^{-6}m^3/s$, which is determined by considering the requirement of laminar flow, restriction of excess hydrostatic pressure and acceptable range of fines loss. It may be argued that a constant inflow rate could not reflect the real hydraulic conditions in dams, which is a limitation of the apparatus. The seepage tests would be terminated at least after 3 hours. At most circumstances, the post-suffusion B-value is larger than 0.93 because of the maintenance of back pressure on the tested specimens. The axial displacement, radial deformation and cumulative eroded fines mass are recorded to determine the fines content and post-suffusion void ratio, which are of significance for the assessment of mechanical responses. After the seepage test, a series of monotonic compression test is performed on the suffusional soil without changing the cell pressure and the back pressure to investigate the mechanical consequences of suffusion. The compression test, either drained or undrained test, is displacement controlled with an axial strain rate of 0.1%/min, following the standard criteria (ASTM D4767-11; ASTM D7181-11). The cell pressure is maintained constant while the specimens are compressed at the designated strain rate.

Mechanical influences of Silica No.8

It is universally recognized that the presence of nonplastic fines creates a “metastable” soil structure, which fundamentally alters the soil mechanical response at shearing from that of clean sand. However, regarding the mechanical function of those nonplastic fines debates still exist. In this paper, the tested soil mixtures contain amounts of nonplastic fine grains, Silica No.8, up to 35% in mass ratio. The mechanical effects of Silica No.8 are elaborated first and further mechanical behavior of soil before and after suffusion could be compared directly.

Figure 3 plots the relations of axial strain and deviator stress, and the corresponding effective stress paths in p'-q diagram of the specimens with the fines contents of 35%, 25%, 15% and 0%, respectively, under an initial effective confining pressure of 50kPa, in the triaxial compression tests under undrained condition. The skeleton sand consists of the coarse Silica No.3 sand, whereas Silica No.8 serves as nonplastic fine grains. The reconstituted specimens with fine grains are prepared by moist tamping method with an initial relative density of approximate 47%. The moist tamped specimen of Silica No.3 is targeted at the largest achievable void ratio to accentuate its dilative tendency even at loose condition. Details of those specimens have been listed in Table 2. It is obviously noted that the presence of Silica No.8 would decrease the soil strength, which may be attributed to the lubrication between skeleton grains by the nonplastic fine grains, thereby smoothing the contacts among the coarse grains. The loss of effective contacts may result in smaller soil stiffness and larger compressibility. Thevanayagam and Mohan (2000) and Thevanayagam (2007) noted similar evidences of the existence of the lubricated soil structures. In terms of effective stress paths, the specimen with 35% fines content displays fully contractive behavior, whereas the soil with less fines content becomes more dilative. Loose though, Silica No.3 without fine grains exhibits fully dilative behavior throughout the compression. It is possible that for the specimen containing 35% fine grains the coarse grains are separated apart by the relatively large amounts of loose fine grains and the contractive behavior may be determined by the compressibility of the fine grains deposited between the coarse grains. With the declining of fines content, the coarse grains gradually contact with each other. The compression may force the fine grains to slide into the voids and correspondingly the coarse grains move into a better contact, causing dilatancy at larger axial strain. In sum, the presence of Silica No.8 decreases the soil strength and inhibits the dilatancy tendency.

Test results and discussions

Summary of seepage test results

A concise summary of the seepage test results is presented for a fundamental understanding of suffusion mechanism and its influence on the soil state. The seepage tests are performed by assigning seepage fluid at a constant rate downwardly through the tested specimens by a flow pump. The flow velocity, defined as the flow volume passing through unit area in unit time, is sufficiently slow in the tests to guarantee a laminar flow condition. In the tests, the flow velocity is gradually increased until it reaches the prescribed value of $5.17\times10^{-6}m^3/s$. Before the onset of suffusion, without any fine grains loss, the hydraulic gradient keeps stable. Once the Darcy velocity reaches critical velocity, the dislodgement of fine grains initiates and correspondingly hydraulic gradient would drop, resulting in an increase in hydraulic conductivity. Successive rising of Darcy velocity may further accelerate the progress of suffusion and correspondingly, large amounts of fine grains would be dislodged, resulting in the contractive deformation of the tested specimens. If the imposed flow rate is kept constant at a value larger than critical velocity for a long period, the loss of fine grains would gradually become constant, indicating the gradual decreasing of erosion rate. Along with the loss of fine grains, coarse fractions may re-arrange their inter-position to reach a new equilibrium and the volumetric deformation will cease. As a result, the tested specimens will become loose. A summary of the changes of hydraulic parameters is indicated in Table 3.

The suffusional behavior of tested specimens is closely dependent on the hydraulic conditions. In authors' tests, the assignment of seepage flow is realized by gradually raising the inflow rate up to $5.17\times10^{-6}m^3/s$ and maintaining this rate till several indicators become stable, such as hydraulic gradient, cumulative eroded soil mass and volumetric strain. Evolution of percentage of cumulative fines loss with time under different initial effective confining pressures and initial fines contents is summarized in Figs. 4 and 5, respectively. It is noted that for each case at the constant imposed flow rate soil experiences an initially sharp loss of fine grains and gradual decreasing of erosion rate with time. The cumulative eroded soil mass is larger under the smaller initial effective confining pressure and is larger for the specimens with the larger initial fines content within the test range. The changes in fines content and void ratios are summarized in Table 3, where the intergranular void ratio is derived by regarding the volume of fine grains as that of voids. It is indicated that with the significant loss of fine grains, the post-suffusion void ratios of tested specimens greatly increase. Although different in the fines loss and post-suffusion void ratio, the suffusional specimens with an initial fines content of 35% show similar intergranular void ratios, averagely equaling to 1.3, which might be a practical comparison base for interpreting the suffusional soil behavior for this study. The evolution of soil state induced by suffusion is plotted in void ratio

~ fines content space (Fig. 6). The post-suffusion specimens have significantly large void ratio, even larger than the maximum void ratio, and thus an extremely loose soil packing is expected. A larger fines content and a smaller void ratio is observed for the specimens on which seepage tests are performed under larger initial effective confining pressure, compared with the specimens under lower initial effective confining pressure. Thevanayagam and Mohan (2000) divided the mechanical behavior of the "coarse domain" soil mixture by a demarcation line corresponding to $e_s \approx e_{cmax}$ (maximum void ratio of the coarse fractions) (Fig. 6). The positions of tested specimens are all above the demarcation line, indicating that the packing of coarse grains is unstable and separated by fine grains, and the soil behavior is affected by those active fine grains participating in the force chains. Due to the characteristics of suffusion, local clogging or accumulation of fine grains might occur and consequently, a particular packing of soil grains might be formed. Therefore, the drained responses of suffusional soils may be different from that of the soil before suffusion.

Influence of initial effective confining pressure on mechanical response of suffusional soil

As is discussed above, a lower effective confining pressure during suffusion would result in larger volumes of voids in soil and more fines loss, and consequently, the mechanical behavior of suffusional soil may be closely related with the confining pressure when suffusion occurs. To reveal this relation, three drained compression tests have been conducted on the suffusional specimens that initially contain 35% fine grains and have suffered suffusion under the same initial effective confining pressure of 50kPa, 100kPa and 200kPa, respectively. Although the post-suffusion void ratios vary for different specimens, the intergranular void ratios are basically equal (i.e., approximately 1.3). If the intergranular void ratio is accepted as the effective reference for the comparison of the mechanical behavior of suffusional soils, the differences in the drained response may be mainly caused by the initial effective confining pressure and the corresponding particular post-suffusion packing of soil grains. The relation curves of deviator stress and axial strain accompanied with the evolution of volumetric strain are plotted in Fig. 7, respectively, which indicate a typical contractant volumetric behavior of loose sand. The deviator stress gradually develops and maintains constant at a peak value, whereas the contractive volumetric strain rises to maximum and keep constant. A majority of experimental investigations has revealed that an axial strain of 30% ~ 40% is necessary for achieving critical state of sand in drained test. Unfortunately, the tests in this study were terminated at the axial strain of about 13% ~ 17%, which should not be sufficiently large to present the full drained responses of suffusional specimens. To compensate the limitation of insufficient straining and depict the whole picture of drained behavior, a hyperbolic curve fitting is adopted to approximate the contractant soil behavior at drained condition (Ferreira and Bica, 2006) and the extrapolated curves up to an axial strain of 40% are shown in Fig. 7 by dash lines. It is worth to mention that the dash lines derived from hyperbolic curve fitting are hypothetical. But considering the significantly large initial void ratio of suffusional specimens, the fitting may reflect the drained behavior appropriately. For comparison purpose, results of drained tests on the companion specimens (35N-50, 35N-100 and 35N-200) under the same stress state as that of suffusional soil are plotted in Fig. 8. The intergranular void ratio of companion specimens is around 1.4, slightly larger than that of the suffusional soil. Herein, failure is defined as the soil state wherein the deviator stress obtained at an axial strain of 15% (ASTM D4767-11; ASTM D7181-11) and correspondingly, the soil strength refers to the deviator stress at an axial strain of 15%. Figure 9 displays the stress ratio at failure, ratio of deviator stress to current mean effective stress, against the initial effective confining pressure, indicating that the soil strength decreases after suffusion and the extent of decreasing becomes smaller at larger initial effective confining pressure. It can be explained that under larger initial effective confining pressure, less fine grains would be dislodged by seepage flow and consequently less changes occurred in the packing of soil grains, resulting in less drop in soil strength after suffusion. In terms of the volumetric strain at failure in Fig. 10, the patterns of behavior of companion specimens are in accordance with the common sense: because of the dilatancy tendency soil commonly fails at smaller volumetric strain under smaller effective confining pressures, and the greater contractive behavior is expected under larger effective confining pressures. However, a different response, departing from common sense, is observed for the suffusional specimen: volumetric strain at failure is larger under lower initial effective confining pressure and it becomes smaller under larger initial effective confining pressure. It can be understood that under lower initial effective confining pressure, more fine grains are eroded away and greater increment in void ratio occurs, and correspondingly at the subsequent compression, for specimen 35E-50, the effect of void ratio increment may surpass that of the dilatency tendency under lower effective confining pressure. Consequently, larger volumetric strain at failure is observed at low initial effective confining pressure.

To fully interpret the reduction of soil strength after suffusion, the critical friction angle is estimated. In this study, the critical state might not be reached at an axial strain of 13% ~ 17% where compression tests are terminated and extrapolation of the data is necessary. The identification of critical state is fulfilled by plotting the stress ~ dilatancy relation of the drained tests on suffusional and companion specimens, and extending the curve to the point of intersection with the zero dilatancy axis. An unique critical stress ratio $(q/p')_{cs}$ could be evaluated as 1.64 and 1.74 for the suffusional and the companion specimens, and accordingly, the derived critical friction angle is 40.1° and 42.4°, respectively. Due to suffusion, the critical friction angle decreases by 5.7%. It may be argued that as an intrinsic physical property critical friction angle should be constant regardless of the change of void ratio after suffusion. However, accompanying with void ratio variation, fines content of suffusional specimens have been significantly reduced, which may cause the reduction of critical friction angle. Further experimental investigations on relative angularity of tested grains might be beneficial to explain the change of friction angle, which might beyond the scope of the study.

Besides, a temporary declining in soil stiffness at the initial stage of shearing with respect to the axial strain ranging from 0% ~ 1% is observed. Figure 11 displays the variation of secant stiffness at the initial 1% of axial strain. The soil stiffness has been normalized by the current mean effective stress in order to compare the cases with different effective confining pressures and accentuate the uniqueness of suffusion induced packing of soil grains. For the comparison purpose, the secant stiffness of the companion specimens is superimposed. Since the companion specimens are similar in terms of the initial fines content and void ratio, the variation of normalized secant stiffness with axial strain displays identical patterns of behavior. The stiffness shows the initially largest value and declines with further compression. However, the behavior pattern of the suffusional specimens is distinct from the companion specimens in three aspects. Firstly, the initial secant stiffness becomes larger than that of the companion specimens, which may be explained by the reinforced soil packing created by suffusion. It is postulated that fine grains may probably be impeded and gradually accumulate at the spots where the size of the pore tunnels, formed by coarse grains, is less than that of the fine grains. At subsequent compression, those fine grains function as jamming rather than lubrication, and thereby reinforcing the packing of soil grains. Secondly, temporary drops in soil stiffness are observed for suffusional specimens 35E-50, 35E-100 and 35E-200, at the axial strain of 0.5%, 0.4% and 0.2%, respectively. It is considered as the evidence of the deterioration of the temporary reinforced soil packing with further straining. Under larger effective confining pressure, the reinforcement may be easily destroyed and therefore, the stiffness drop in specimen 35E-200 is found at lower axial strain. Thirdly, because of the extremely loose state of the suffusioanl specimens, the normalized secant stiffness keeps lower than that of the companion specimens after the stiffness drop.

Influence of initial fines content on mechanical response of suffusional soil

Differences in initial fines content directly result in a different soil packing before suffusion, which will exert an influence on the progress of suffusion and the post-suffusion soil packing. As is shown in Fig. 5, a larger amount of fines loss is observed at the specimen with larger initial fines content. An understanding of the effects of initial fines content may shed light on the evolution of soil packing during suffusion and mechanical responses of suffusional soil. The analysis below is limited to the tests under an initial effective confining pressure of 50kPa, which show the largest increment in void ratio and drop in soil strength.

In a specimen, a fraction of fine grains fill the voids, whereas another fine grains separate the coarse grains. Since the fine grains occupying the voids among the coarse grains may hardly participate in force chains (Skempton and Brogan, 1994), the fine grains in the voids may be vulnerable to suffusion and probably dislodged by seepage flow. Erosion of the fine grains effectively separating the coarse grains may occur at larger Darcy's flow and the rearrangement of coarse grains occurs to reach new equilibrium. Majority of the "surviving" fine grains after three-hour seepage test are wedged between coarse grains and actively participating in the force chains. Because of the larger voids size among coarse grains of the specimen with 35% initial fines content (specimen 35E-50) compared with other specimens (specimen 25E-50 and 15E-50), if the relative density is similar and fine grains are merely considered as voids, specimen 35E-50 may show larger loss of fine grains. Under the same initial effective confining pressure of 50kPa, different although the initial fines content is, the specimens show approximately similar post-suffusion fines content (i.e., 10%~13%) but different post-suffusion void ratios, as is shown in Table 3. Because of the obvious differences in post-suffusion void ratio, the drained responses of those suffusional specimens should be different. Figure 12 shows the results of drained compression test on specimen 35E-50, 25E-50 and 15E-50 under an initial effective confining pressure of 50kPa. Specimen 35E-50, which is the largest in post-suffusion void ratio, exhibits the lowest soil strength and secant stiffness. In terms of volumetric strain, three specimens show similar amounts of contractive strain within the initial 6% axial strain. Afterwards, specimen 15E-50, which is the smallest in post-suffusion void ratio, become dilative at an axial strain of 14%, and similarly specimen 25E-50 exhibiting dilatancy at an axial strain of 19%. Specimen 35E-50 does not show dilative behavior within test range.

Distinctive packing of soil grains after suffusion

Monotonic compression tests have revealed the somewhat different soil responses of the suffusional soil: under the larger initial effective confining pressure it exhibits a less volumetric strain and a temporal decline in soil secant stiffness is observed within the initial 1% axial strain. Since the intergranular void ratio of the suffusional specimens are approximately the same and the effective confining pressure may not be sufficiently large to trigger grain crushing (i.e., a maximum initial effective confining pressure of 200kPa), the soil responses should be dominated by the post-suffusion soil packing and the soil grain movement during shearing.

To signify the distinguished packing of soil grains after suffusion, monotonic drained test on a reconstitute specimen with similar fines content and initial void ratio as that of suffusional specimen 35E-50 is performed. The reconstituted specimen with an initial fines content of 15% is prepared by moist tamping method, targeting at the largest achievable void ratio. Because of the occurrence of large volumetric deformation during consolidation, the void ratio before compression is 0.81, still less than the post-suffusion void ratio of 1.0 for specimen 35E-50. Figure 13 shows the drained responses of the two specimens in terms of stress ~ strain relationship and corresponding development of volumetric strain. Due to the larger void ratio, the suffusional specimen mostly gains less strength. However, careful examination of the stress ~ strain curves within the initial 1% axial strain shows that the initial secant stiffness of suffusional specimen is larger than that of the reconstituted specimen and a sudden drop in deviator stress is observed around 0.5% axial strain, after which soil strength and secant stiffness keep smaller than those of the reconstituted specimen throughout the test range.

The above test suggests a distinguished packing of soil grains after suffusion, different from reconstituted fine-grains-containing sand. Specifically, compared with the denser reconstituted specimens, the suffusional specimen still becomes much stiffer at the beginning of shearing. It is inferred that along with the seepage flow amounts of fine grains keep being dislodged and coarse grains rearrange their positions into a new equilibrium. Because of possible clogging, fine grains might be accumulated at the spots where the constriction size, representing the size of pore channels in a soil, is smaller than that of fine grains. Due to the rearrangement of grains, those accumulated fine grains may actively participate in force chains. Different from the function of “lubrication”, those “surviving” fine grains after suffusion would probably perform like reinforcement or jamming. Thereafter, the reinforced post-suffusion soil packing renders the suffusional specimen much stiffer and less compressible at the beginning of shearing. With the subsequent compression the reinforcement is deteriorated and the suffusional specimen may behave like typical fine-grains-containing sand. To further validate this assumption, a microscopic observation of the post-suffusion packing of soil grains might be necessary.

Conclusions

The mechanical consequences of suffusion on a series of cohesionless soils are presented in this paper. The tested specimens consist of the binary mixtures of Silica sand No.3 and No.8. With larger grain size, Silica No.3 works as the soil skeleton, whereas Silica No.8 is the erodible fine grains. Mechanically, the presence of Silica No.8 would decrease the soil strength and inhibit the dilatancy tendency of Silica No.3, which may be due to the lubrication function of the nonplastic Silica No.8 deposited between the skeleton grains. By utilizing the modified triaxial permeameter, seepage tests are performed on those specimens to create suffusion condition, and drained monotonic compression tests are performed on the suffusional specimens to reveal their mechanical behavior.

Soil strength decreases after suffusion and the amounts of drops become smaller under larger initial effective confining pressure. Departing from the pattern of behavior of the companion specimen, the suffusional soil behaves differently: its volumetric strain at compression is larger under lower initial effective confining pressure and it becomes smaller under larger initial effective confining pressure. In terms of soil stiffness, the initial secant stiffness of suffusional soil becomes larger than that of the companion soil and a temporary drop in soil stiffness at the initial stage of shearing with respect to the axial strain ranging from 0% ~ 1% is observed. It may be regarded as the evidence of the deterioration of the temporary reinforced soil packing with further straining and that reinforcement may be easily destroyed under larger initial effective confining pressure.

Under the same initial effective confining pressure of 50kPa, the specimen with larger initial fines content shows a larger amount of fine grains loss during the seepage test, resulting in a larger post-suffusion void ratio. At the subsequent compression, this specimen would exhibit lower soil strength and secant stiffness.

Compression test results have revealed the probable existence of a distinctive packing of soil grains after suffusion. The “surviving” fine grains after suffusion may actively participate in the force chains, acting like reinforcement. The reinforced post-suffusion soil packing renders the suffusional specimen much stiffer and less compressible. With the subsequent compression the reinforcement will be deteriorated and the suffusional specimen may behave like typical fine-grains-containing sand.

Acknowledgement

The first author acknowledges the Japanese Government (Monbukagakusho: MEXT) scholarship support for performing this research. This work was supported by JSPS KAKENHI Grant Numbers 25420498.

References

ASTM D2487-11. (2012). “Standard Practice for Classification of Soils for Engineering Purposes (Unified Soil Classification System).” *Annual Book of ASTM Standards,* Vol.04.08, ASTM International, West Conshohocken.

ASTM D4767-11. (2012). “Standard Test Method for Consolidated Undrained Triaxial Compression Test for Cohesive Soils.” *Annual Book of ASTM Standards,* Vol.04.08, ASTM International, West Conshohocken.

ASTM D7181-11. (2012). “Method for Consolidated Drained Triaxial Compression Test for Soils.” *Annual Book of ASTM Standards,* Vol.04.09, ASTM International, West Conshohocken.

Chang, C.S., and Meidani, M. (2012). “Deformation and failure behavior of soils under erosion.” *Poster of NSF CMMI Engineering Research and Innovation Conference, Boston, MA, USA*, CMMI-0928433.

Chang, D.S., and Zhang, L.M. (2011). “A stress-controlled erosion apparatus for studying internal erosion in soils.” *Geotechnical Testing Journal*, 34(6), 579-589.

Cubrinovski, M., and Ishihara, K. (2002). “Maximum and minimum void ratio characteristic of sands.” *Soils and Foundations*, 42(6), 65-78.

Ferreira, P.M.V., and Bica, A.V.D. (2006). “Problems in identifying the effects of structure and critical state in a soil with a transitional behaviour.” *Géotechnique*, 56(7), 445-454.

Hicher, P.-Y. (2013). “Modelling the impact of particle removal on granular material behavior.” *Géotechnique*, 63(2), 118-128.

Jiang, M.J., Konrad, J.M., and Leroueil, S. (2003). “An efficient technique for generating homogeneous specimens for DEM studies.” *Computers and Geotechnics*, 30(7), 579-597.

Kezdi, A. (1979). *Soil Physics: Selected Topics (Developments in Geotechnical Engineering),* Elsevier Science Ltd., Amsterdam, Netherlands.

Ke, L., and Takahashi, A. (2012). “Strength reduction of cohesionless soil due to internal erosion induced by one-dimensional upward seepage flow.” *Soils and Foundations*, 52(4), 698-711.

Ke, L., and Takahashi, A. (2014). “Triaxial erosion test for evaluation of mechanical consequences of internal erosion.” *Geotechnical Testing Journal*, 37(2), 347-364.

Lade, P.V., Liggio, C.D., Jr., and Yamamuro, J.A. (1998). “Effects of non-plastic fines on minimum and maximum void ratios of sand.” *Geotechnical Testing Journal*, 21(4), 336-347.

Muir Wood, D., Maeda, K., and Nukudani, E. (2010). “Modeling mechanical consequences of erosion.” *Géotechnique*, 60(6), 447-457.

Skempton, A.W., and Brogan, J.M. (1994). “Experiments on piping in sandy gravels.” *Géotechnique*, 44(3), 449-460.

Sugita, H., Sasaki, T., and Nakajima, S. (2008). “Damage investigation of road embankment caused by the 2007 Noto Peninsula, Japan Earthquake.” *Public Works Research Institute Report.*

Thevanayagam, S., and Mohan, S. (2000). “Intergranular state variables and stress-strain behavior of silty sands.” *Géotechnique*, 50(1), 1-23.

Thevanayagam, S. (2007). “Intergrain contact density indices for granular mixes - Ⅰ : Framework.” *Earthquake Engineering and Engineering Vibration*, 6(2), 123-134.

Xiao, M., and Shwiyhat, N. (2012). “Experiment investigation of the effects of suffusion on physical and geomechanic characteristics of sandy soils.” *Geotechnical Testing Journal*, 35(6), 1-11.

Table 1 Physical properties of tested soils

Physical properties	Silica No.3	Silica No.8	Mixtures with 35% Silica No.8	Mixtures with 25% Silica No.8	Mixtures with 15% Silica No.8
Fines content (*FC*) (%)	---	---	35	25	15
Maximum void ratio	0.94	1.33	0.74	0.77	0.79
Minimum void ratio	0.65	0.70	0.36	0.37	0.53

Table 2 Details of tested specimens

Specimens	Initial *FC* (%)	Initial void ratio (e_i)	Mean effective stress at consolidation (kPa)	Post consolidation void ratio (e_c)	Relative density (%)	Type of compression
35E-50	35.0	0.59	50	0.55	48.5	Drained
35E-100	35.0	0.60	100	0.56	47.5	Drained
35E-200	35.0	0.64	200	0.57	46.2	Drained
25E-50	25.0	0.61	50	0.60	42.8	Drained
15E-50	15.0	0.68	50	0.68	43.1	Drained
35N-50	35.0	0.59	50	0.55	48.5	Drained
35N-100	35.0	0.61	100	0.56	47.5	Drained
35N-200	35.0	0.59	200	0.54	51.1	Drained
35U-50	35.0	0.60	50	0.56	47.5	Undrained
25U-50	25.0	0.61	50	0.58	47.8	Undrained
15U-50	15.0	0.68	50	0.67	46.9	Undrained
0U-50	0.00	0.88	50	0.88	21.8	Undrained

Note: Specimens named with “E” means seepage tests have been performed on the specimens at a constant inflow rate of $5.17\times10^{-6}\mathrm{m}^3/\mathrm{s}$, whereas those with “N” indicate the companion specimens without suffusion. Those specimens named with “U” are prepared for study of mechanical influence of fine fraction.

Table 3 Summary of soil states after suffusion/before compression

Specimen	$i_{max}^{(1)}$	$k_i^{(2)}$ (m/s)	$k_e^{(3)}$ (m/s)	$FC^{(4)}$ (%)	$e_e/e_c^{(5)}$	$e_s^{(6)}$
35E-50	11.7	9.7×10^{-5}	0.028	13.5	1.0	1.29
35E-100	7.17	1.0×10^{-4}	0.010	15.9	0.92	1.29
35E-200	10.5	1.0×10^{-4}	0.008	24.5	0.77	1.34
25E-50	5.05	1.0×10^{-4}	0.009	12.0	0.81	1.06
15E-50	2.07	1.2×10^{-4}	0.010	9.98	0.78	0.98
35N-50	---	---	---	35.0	0.55	1.39
35N-100	---	---	---	35.0	0.56	1.40
35N-200	---	---	---	35.0	0.54	1.37

Note: (1) Maximum hydraulic gradient, i_{max};
(2) Initial hydraulic conductivity before suffusion, k_i (m/s);
(3) Post-suffusion hydraulic conductivity, k_e (m/s);
(4) Fines content after suffusion/before compression for suffusional specimens and initial fines content for companion specimens, FC (%);
(5) Void ratio after suffusion/before compression for suffusional specimens, e_e and post-consolidation void ratio for companion specimens, e_c;
(6) Intergranular void ratio $e_s=(e_e+FC/100)/(1-FC/100)$ (suffusional specimens) and $e_s=(e_c+FC/100)/(1-FC/100)$ (companion specimens).

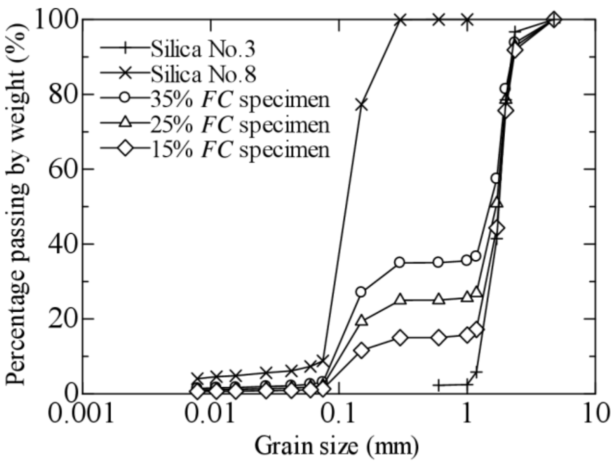

Fig. 1. Grain size distributions (FC indicates fines content)

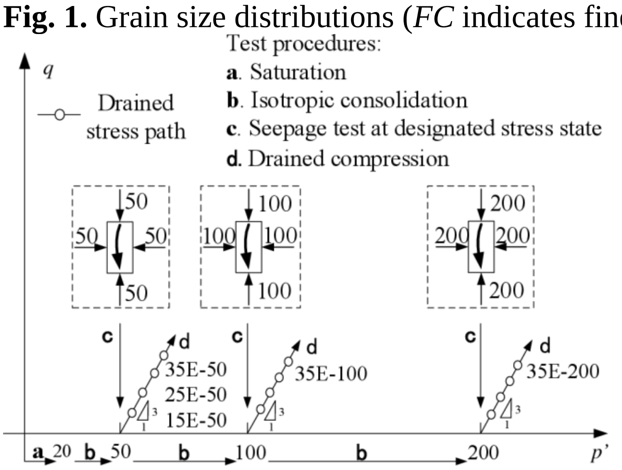

Fig. 2. Schematic diagram of test procedures in p'-q space with test cases

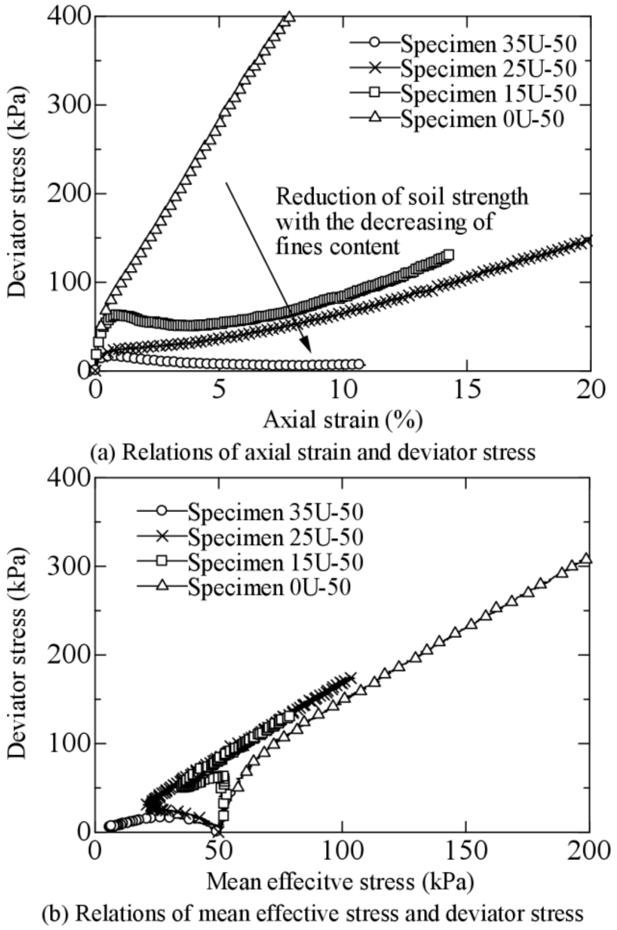

Fig. 3. Undrained compression tests on specimens with different contents of Silica No.8 under an initial effective confining pressure of 50kPa

(a) Relations of axial strain and deviator stress

(b) Relations of mean effective stress and deviator stress

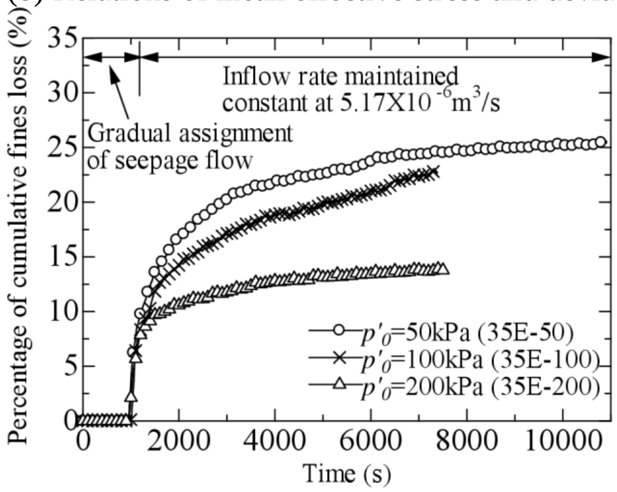

Fig. 4. Cumulative eroded soil mass with time for specimens with 35% initial fines content under different initial confining pressures

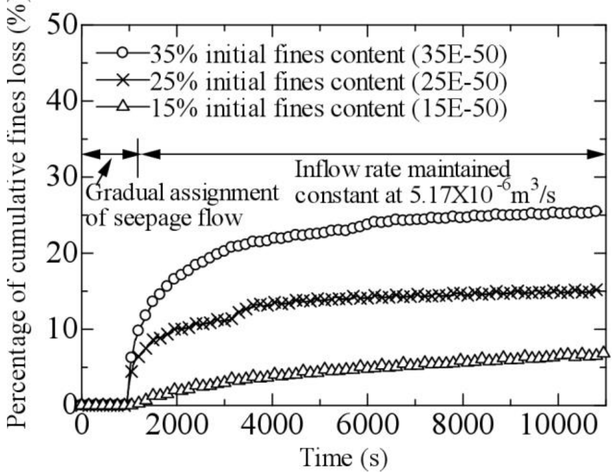

Fig. 5. Cumulative eroded soil mass with time for specimens tested under an initial effective confining pressure of 50kPa

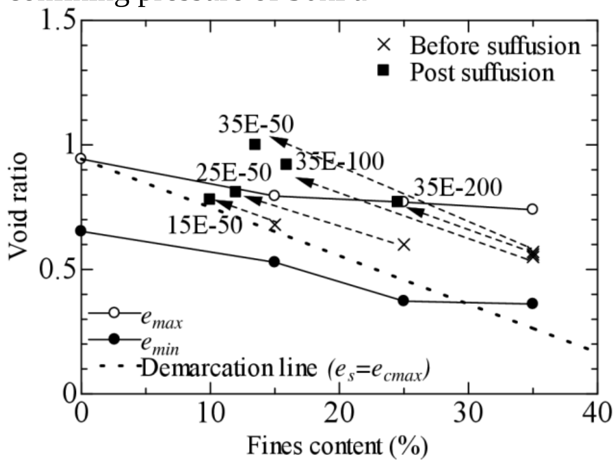

Fig. 6. Changes of soil state induced by suffusion in fines content ~ void ratio space

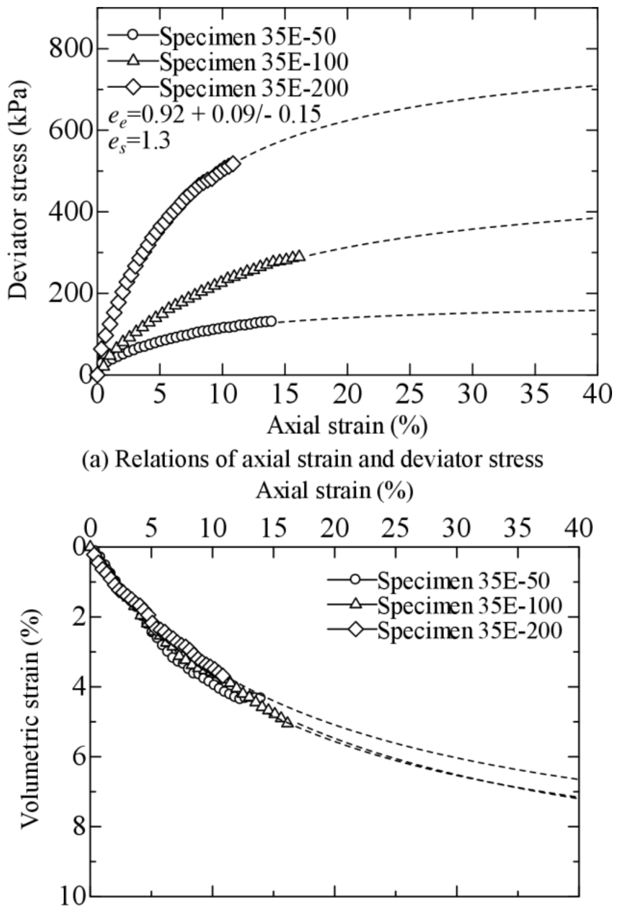

(a) Relations of axial strain and deviator stress

(b) Relations of axial strain and volumetric strain

Fig. 7. Drained compression tests on suffusional specimens under different initial effective confining pressures (Dash lines indicate the extrapolated curve by a hyperbolic fitting)
(a) Relations of axial strain and deviator stress
(b) Relations of axial strain and volumetric strain

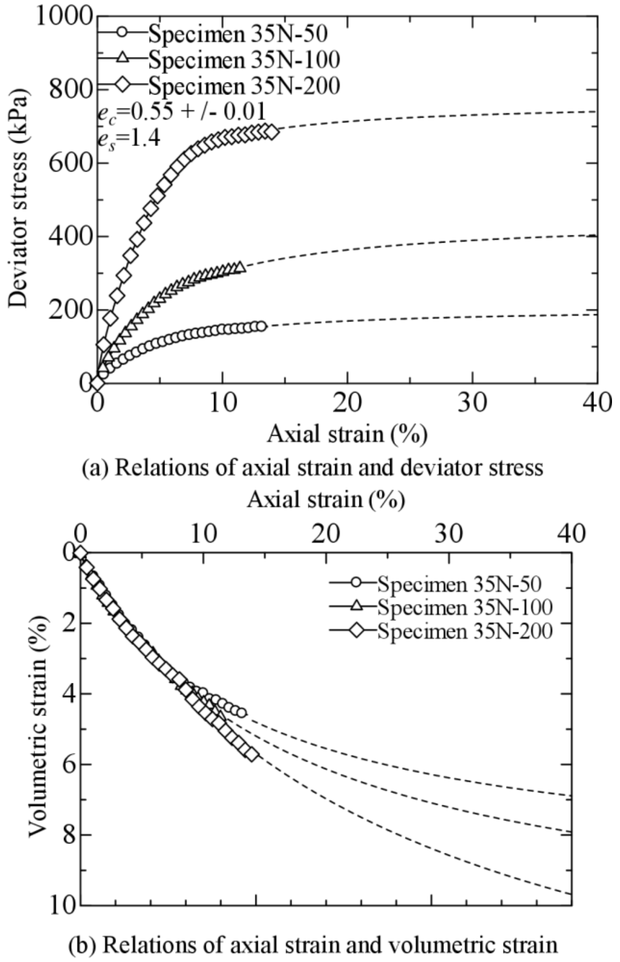

Fig. 8. Drained compression tests on companion specimens under different initial effective confining pressures (Dash lines indicate the extrapolated curve by a hyperbolic fitting)
(a) Relations of axial strain and deviator stress
(b) Relations of axial strain and volumetric strain

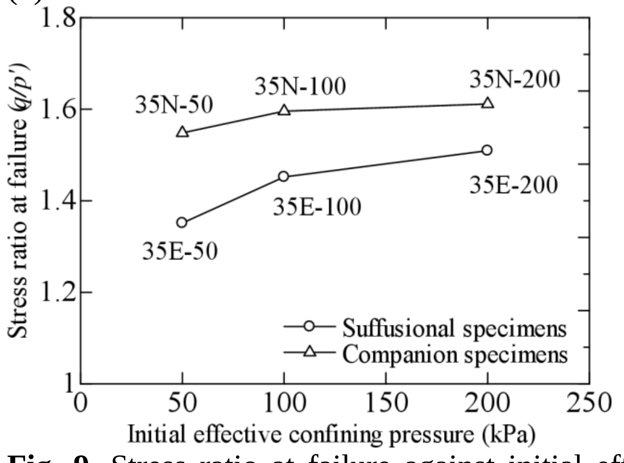

Fig. 9. Stress ratio at failure against initial effective confining pressure (refer Table 3 for details of specimens conditions)

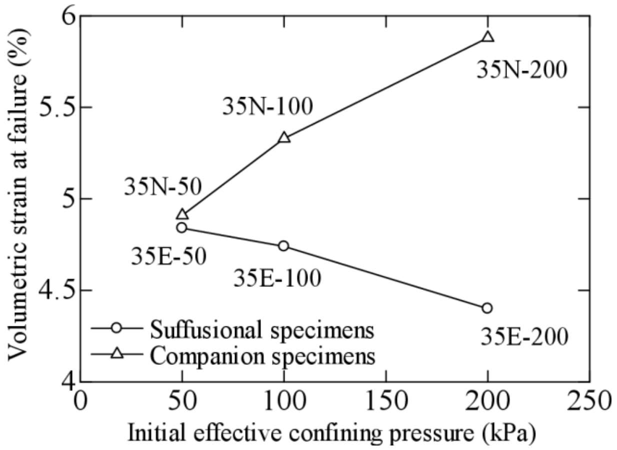

Fig. 10. Volumetric strain at failure against initial effective confining pressure (refer Table 3 for details of specimens conditions)

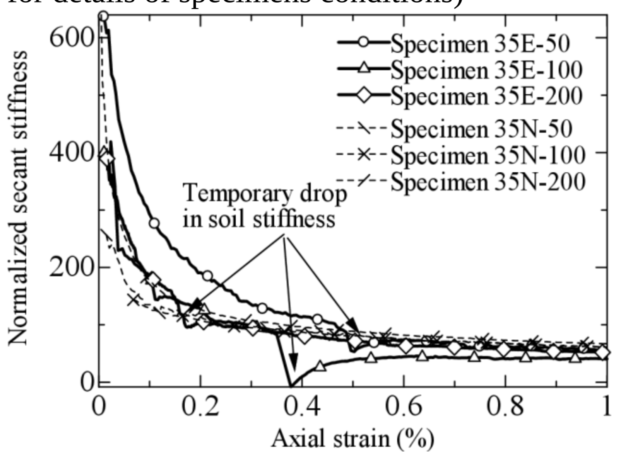

Fig. 11. Normalized secant stiffness within 1% of axial strain

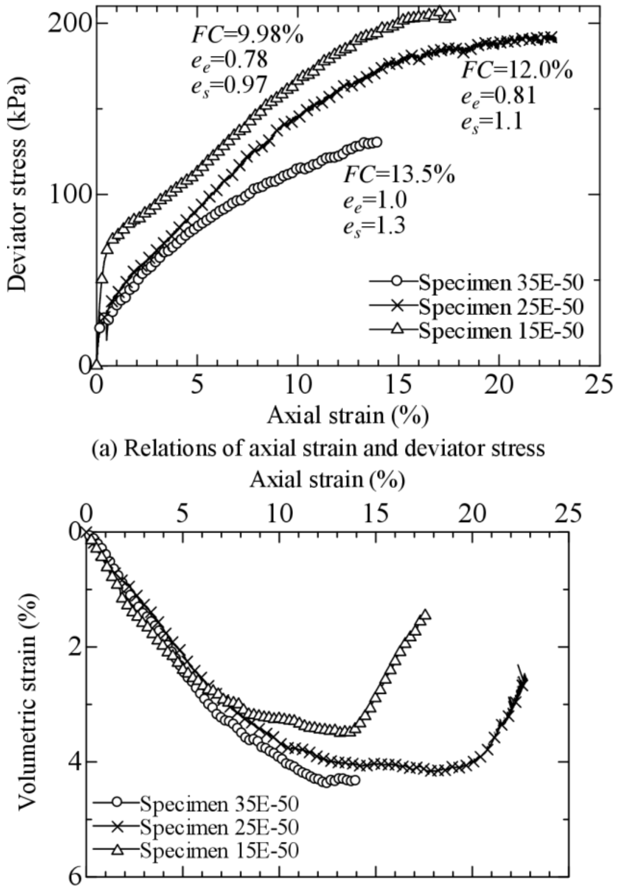

(a) Relations of axial strain and deviator stress

(b) Relations of axial strain and volumetric strain

Fig. 12. Drained responses of suffusional specimens with different initial fines contents under an initial effective confining pressure of 50kPa
(a) Relations of axial strain and deviator stress
(b) Relations of axial strain and volumetric strain

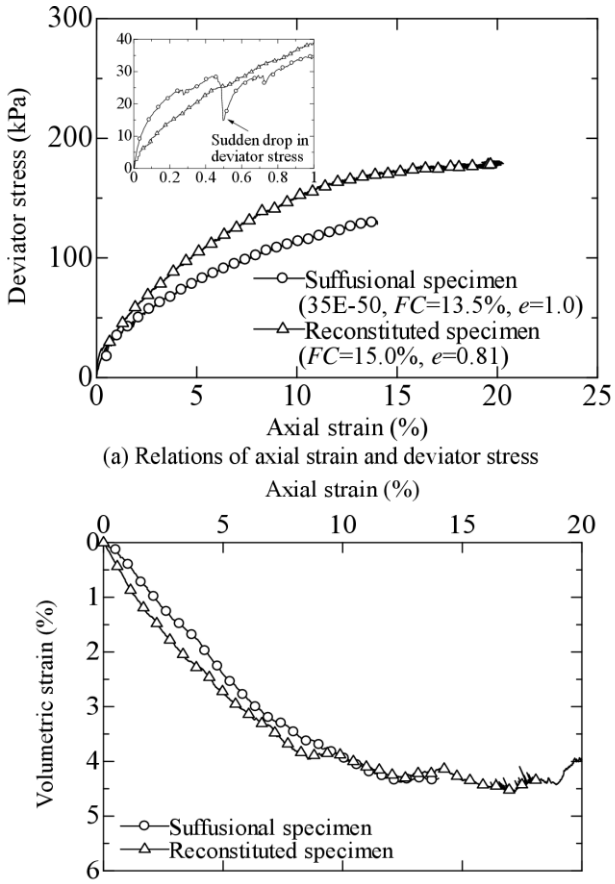

(b) Relations of axial strain and volumetric strain

Fig. 13. Drained responses of suffusional specimen and reconstituted specimen under an initial effective confining pressure of 50kPa

(a) Relations of axial strain and deviator stress

(b) Relations of axial strain and volumetric strain